HETEROCYCLES, Vol. 89, No. 5, 2014, pp. 1173 - 1181. © 2014 The Japan Institute of Heterocyclic Chemistry
Received, 17th February, 2014, Accepted, 26th March, 2014, Published online, 7th April, 2014
DOI: 10.3987/COM-14-12963

SYNTHESIS AND PHOTOPHYSICAL PROPERTIES OF DIKETOPYRROLOPYRROLE-BASED NEAR-INFRARED DYES

Takuya Yamagata, Junpei Kuwabara, and Takaki Kanbara*

Tsukuba Research Center for Interdisciplinary Materials Science (TIMS), Graduate School of Pure and Applied Sciences, University of Tsukuba, 1-1-1 Tennodai, Tsukuba 305-8573, Japan

Abstract – The introduction of phenylethynyl groups to boron-coordinated diketopyrrolopyrrole (DPP) derivatives resulted in the extension of π-conjugation, thereby showing bathochromic shifts of both absorption and emission wavelengths. The emission maximum of the DPP derivatives shifted to a near-infrared region.

INTRODUCTION

Near-infrared (NIR) dyes, which absorb and/or emit light in the region 700–2000 nm, have been utilized in the field of materials sciences.[1] They have also been used as fluorescent probes for biological imaging because the application of NIR light leads to low auto-fluorescence and low light scattering in tissues.[2] Moreover, NIR dyes have been recognized as promising materials in dye-sensitized solar cells.[3]

Boron dipyrromethane (BODIPY)[4] and squaraine-based dyes[5] have been developed as high-performance NIR dyes in recent years. In particular, BODIPY and its analogs have been recognized as promising materials in the field of optoelectronics owing to their high molar absorbance coefficients and high emission quantum yields.[1,6] Alternatively, diketopyrrolopyrrole (DPP) consists of a condensed lactam core flanked by aromatic groups and is a functional dye of increasing interest. DPP has been utilized in organic solar cells,[7] organic thin-film transistors,[8] chemosensors,[9,10] and dye lasers[11] owing to its high carrier mobilities and molar absorbance coefficients. Zumbusch *et al.* recently reported pyrrolopyrrole cyanine type analogs showing strong absorption and emission in the NIR region.[12] Shimizu *et al.* synthesized pyrrolopyrrole aza-BODIPY analogs exhibiting strong emission in the lower-energy visible region.[13] Recently, we reported a simple strategy for absorption and emission of DPP derivatives in long-wavelength region by synthesizing DPP derivatives having coordinate bonds to boron (Figure 1).[14] The resulting coplanar structure formed by the coordinate bonds extended the π-conjugation between the

condensed lactam core and flanked aromatic groups, exhibiting long-wavelength emissions in the region 632–662 nm. The photophysical properties of DPP derivatives strongly depend on the flanked aromatic substituents;[15,16] therefore, further extension of the π-conjugation system is expected to result in emission in the NIR region. For this purpose, we introduced phenylethynyl groups to the boron-coordinated DPP derivatives. Herein, we report the synthesis and evaluation of photophysical properties of DPP derivative-based NIR dyes.

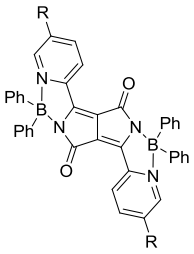

Figure 1. Structure of boron-coordinated diketopyrrolopyrrole (DPP) derivative

RESULTS AND DISCUSSION

DPP derivative **1** was prepared following the literature procedure (Scheme S1 in the Supporting Information).[14] The 4-(dimethylamino)phenylethynyl and 4-methoxyphenylethynyl groups were introduced by the Sonogashira coupling reaction with 2-dicyclohexylphosphino-2′,4′,6′-triisopropylbiphenyl (XPhos) as the ligand to afford the corresponding DPP derivatives **2** and **3** in 49% and 50% yields, respectively (Scheme 1). For comparison, DPP derivatives **4** and **5** were also prepared following the literature procedures (Figure 2).[14,16b]

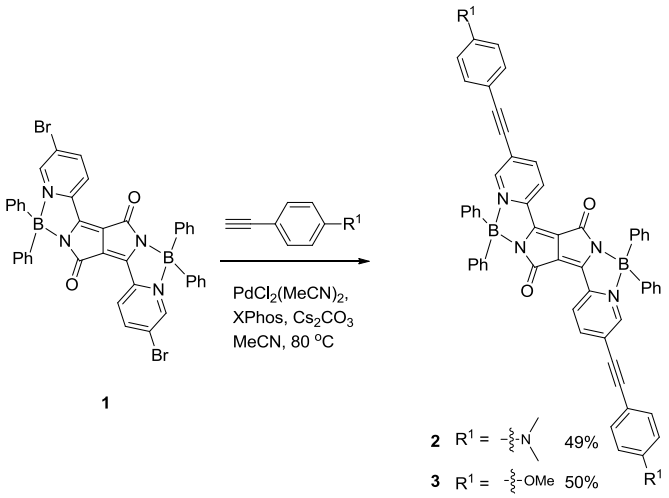

Scheme 1. Syntheses of DPP derivatives **2** and **3**

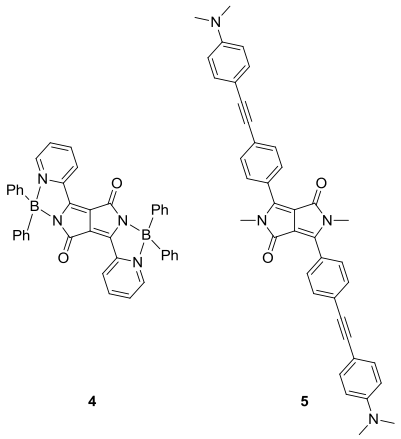

Figure 2. Structures of DPP derivatives **4** and **5**

The photophysical properties of **2** and **3** were evaluated and compared to those of **4** and **5**, and the results are summarized in Table 1. The absorption spectra were measured in chloroform (Figure 3, left). The spectra of **2**–**4** show two vibronic transitions 0-0 and 0-1. Because the vibrational structure was not observed for **5**, the vibrational structures of **2**–**4** were attributed to the rigid coplanar structure of the condensed lactam core (DPP core) and aromatic groups.[17] The maximum absorption wavelength (λ_{max}) of **2** (685 nm) was 68 nm longer than that of **4** (617 nm). This significant bathochromic shift showed that the introduction of 4-(dimethylamino)phenylethynyl groups extended the π-conjugation. Moreover, the λ_{max} of **2** also appeared in a longer wavelength region than that of **3** (667 nm) with 4-methoxyphenylethynyl group presumably because of a higher electron donating ability of the introduced group.[12f] The large bathochromic shift (163 nm) of **2** in comparison to that of **5** indicated a significant effect of the coordination of boron.[14] The molar absorbance coefficient (ε) of **2** was two-fold higher than that of **4**, indicating that the extension of the π-conjugation also contributed to the increase in ε.

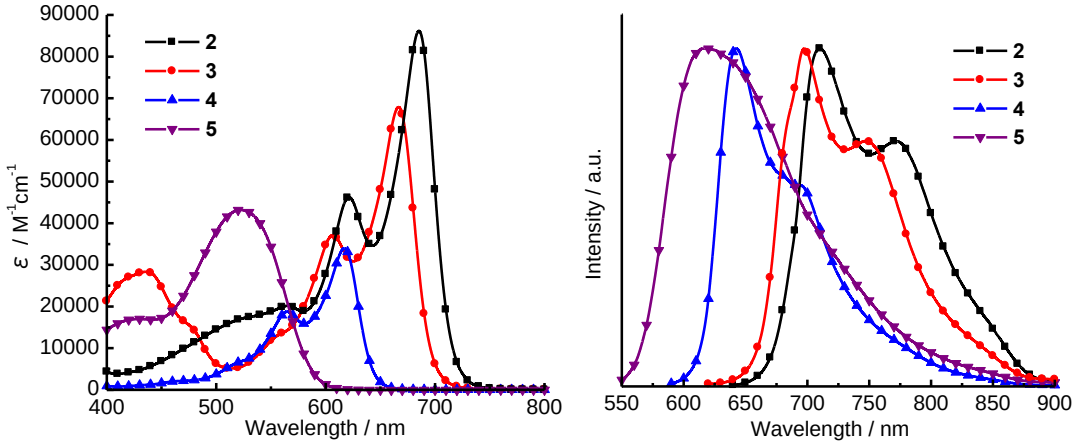

Figure 3. Absorption spectra (left) and normalized emission spectra (right) of DPP derivatives **2**–**5** in chloroform

The emission spectra of **2**–**5** are shown in Figure 3 (right). DPP derivative **2** exhibits the maximum emission (λ_{em}) at 710 nm with a shoulder peak at 771 nm in the NIR region, indicating that the combination of the coordination of DPP to boron and the introduction of 4-(dimethylamino)phenylethynyl group results in the emission in the NIR region. Similarly, the λ_{em} of **3** was close to the NIR region. The order of λ_{em} was the same as that of absorption (**5** < **4** < **3** < **2**). The Stokes shifts of **2** (514 cm^{-1}), **3** (645 cm^{-1}), and **4** (533 cm^{-1}) were smaller than that of **5** (3002 cm^{-1}), indicating that the coordination of DPP to boron results in a rigid planer structure. The moderate emission quantum yield (Φ_f) in the range 0.22–0.72 was observed for **2**–**5**.

Table 1. Photophysical properties of DPP derivatives **2**–**5**

	Absorption[a]		Simulated	Emission[c]	Stokes shift / cm^{-1}	Φ_f[d]
	λ_{max} / nm	ε / $Lmol^{-1}cm^{-1}$	λ_{max}[b] / nm	λ_{em} / nm	in solution	solution
2	685	86200	720	710	514	0.22
3	667	67900	708	697	645	0.53
4	617	34000	639	638	533	0.61
5	522	43200	581	619	3002	0.72

[a] Absorption spectra were measured in chloroform. [b] The wavelengths of maximum absorption simulated by Time-dependent density functional theory (TD-DFT) calculations. [c] Emission spectra were measured with excitation at λ_{max} in chloroform. [d] Absolute fluorescence quantum yields in chloroform.

The relationship between the structures of **2**–**5** and their photophysical properties was also evaluated by theoretical calculations. After the geometry optimization of the structures, time-dependent density theory (TD-DFT) calculations were performed using the Gaussian 09 program suite.[18] The trend in simulated λ_{max} is consistent with the results obtained from the absorption spectra (Table 1), and the values of the calculated energy gaps (E_g^{calcd}) are in good agreement with those of the experimentally obtained optical energy gaps (E_g^{opt}, Table 2). Therefore, the results of theoretical calculations were considered to be reliable, and the absorption properties were evaluated from the results of the theoretical calculations.

Owing to the extension of π-conjugation by the introduction of 4-(dimethylamino)phenylethynyl group, both the highest occupied molecular orbital (HOMO) and the lowest unoccupied molecular orbital (LUMO) energy levels of **2** are higher than those of **4** (Table 2). In particular, the increase in the HOMO level (0.42 eV) is more significant than that of the LUMO level (0.22 eV). Therefore, the extension of π-conjugation caused the high HOMO level, resulting in the narrow energy gap of DPP derivative **2**.

Table 2. HOMO-LUMO energies and energy gaps of DPP derivatives **2**–**5** on the basis of the theoretical calculation [a]

	HOMO	LUMO	E_g^{calcd}	E_g^{opt}
2	-4.82 eV	-2.96 eV	1.72 eV	1.73 eV[b]
3	-4.98 eV	-3.10 eV	1.75 eV	1.78 eV[b]
4	-5.24 eV	-3.17 eV	1.94 eV	1.93 eV[b]
5	-4.63 eV	-2.31 eV	2.13 eV	2.10 eV[b]

[a] TD-DFT calculations were performed at the B3LYP level with the 6-31G(d,p) [b] Estimated by absorption spectroscopy.

Figure 4 shows the molecular orbitals of **2**–**5**. The HOMO of **2** is almost localized on the DPP core, whereas the LUMO of the DPP derivative **2** is extended on the DPP core and the 2-pyridyl groups. Similar trends were observed in the HOMO and LUMO of **3** and **4**. Based on the TD-DFT calculations, the main absorption in the long-wavelength region was attributed to transitions from the HOMO to the LUMO, which were assigned as π–π* transitions (Figure 4 and Table 3). The most remarkable difference between the absorptions of **2** and **3** was the broad absorptions of **2** at ~565 nm (Figure 3, left). According to the results of the TD-DFT calculations, the absorption was attributed to charge transfer (CT) transition from the 4-(dimethylamino)phenyl groups to the DPP core (HOMO−2 to LUMO, Figure 5, and Table 3).[12f,19] Owing to the higher electron-donating ability of the 4-(dimethylamino)phenyl groups, the CT transition (HOMO−2 to LUMO) of **2** is close to the π–π* transitions (HOMO to LUMO).[12f]

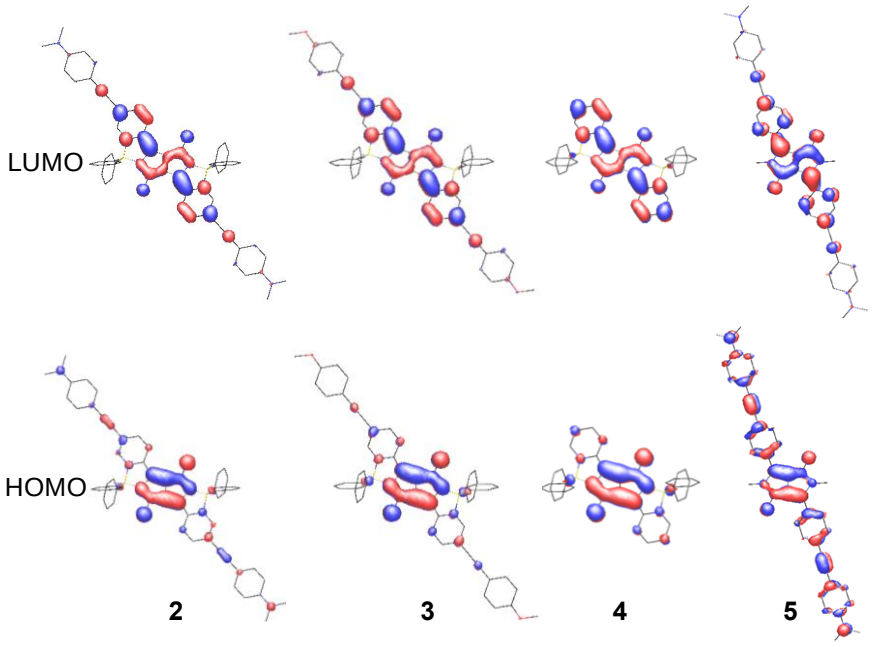

Figure 4. Molecular orbitals of DPP derivatives **2**–**5**

Table 3. List of calculated main electronic transitions of DPP derivatives **2**–**5** in the gas phase

	Simulated λ_{max}	Composition		f^a
2	720 nm	HOMO→LUMO	(0.71)	1.399
	553 nm	HOMO-2→LUMO	(0.70)	0.547
3	708 nm	HOMO→LUMO	(0.71)	1.056
4	639 nm	HOMO→LUMO	(0.58)	0.423
5	581 nm	HOMO→LUMO	(0.70)	1.868

[a] Oscillator strengths.

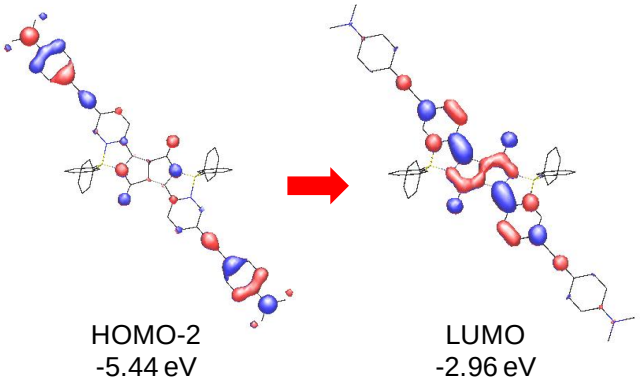

Figure 5. Molecular orbitals of DPP derivative **2**

In conclusion, we synthesized the DPP-based NIR dyes and investigated their photophysical properties. The introduction of 4-(dimethylamino)phenylethynyl group resulted in an extension of π-conjugation in the boron-coordinated DPP derivatives, showing strong absorption in the visible region and emission in the NIR region. Owing to favorable photophysical properties and the straightforward synthetic route, the DPP dyes may be utilized in chemosensors, biological imaging, and photovoltaics upon further modification in the future.

EXPERIMENTAL

Materials

2-Dicyclohexylphosphino-2′,4′,6′-triisopropylbiphenyl (XPhos) was purchased from Sigma–Aldrich. Dichlorobis(acetonitrile)palladium(II) [$PdCl_2(MeCN)_2$] was prepared according to the literature method.[20] Other chemicals were purchased and used without further purification.

General Experimental Procedures

NMR spectra were recorded on Bruker AVANCE-400 and JEOL ECS-400 NMR spectrometers. Absorption spectra were recorded on a JASCO V-630iRM spectrophotometer. Emission spectra were

recorded on a FP-6200 spectrophotometer. Emission quantum yields were obtained by a Hamamatsu Photonics absolute emission quantum yield measurement system C9920-02. MALDI-TOF MS spectra were recorded on Applied Biosystems SCIEX TOF/TOF^{TM} 5800. HRMS (ESI) spectra were recorded on UPLC/Synapt G2 HDMS.

Computational details

The geometrical structures were optimized at the B3LYP level with 6-31G (d,p) basis set implemented in Gaussian 09 programs suits.[18] Using the optimized geometries, TD-DFT calculations were performed to predict their absorptions. Because the calculation of the geometrical structure of **2** did not unspread, the geometrical structure was optimized at the B3LYP level for **2** with 6-31G basis set implemented in Gaussian 09 programs suits.

Synthesis and characterization

DPP derivative 2: A mixture of **1** (23.3 mg, 30 μmol), 4-ethynyl-*N*,*N*-dimethylaniline (21.8 mg, 150 μmol), Cs_2CO_3 (25.5 mg, 130 μmol), $PdCl_2(MeCN)_2$ (0.6 mg, 2.4 μmol) and XPhos (2.3 mg, 4.8 μmol) in MeCN (1.5 mL) was stirred for 10 min at room temperature under nitrogen atmosphere. The mixture was heated at 80 °C for 21 h. After cooling to room temperature, the volatiles were evaporated to dryness in vacuo. A dark blue solid was isolated by column chromatography on silica gel using $CHCl_3$/EtOAc (20/1) as an eluent. The product was obtained by the recrystallization ($CHCl_3$/hexane), and dried under vacuum to obtain a dark blue solid (13.2 mg, 49%). ^{1}H NMR (400 MHz, $CDCl_3$, 298 K) δ 3.03 (s, 12H), 6.64 (d, 4H, J = 9.2 Hz), 7.30-7.33 (m, 12H), 7.39 (d, 4H, J = 9.2 Hz), 7.43 (d, 8H, J = 6.8 Hz), 8.10 (d, 2H, J = 8.4 Hz), 8.40 (d, 2H, J = 8.8 Hz), 8.47 (s, 2H); Carbon peak of **2** was not observed due to low solubility in ^{13}C{^{1}H} NMR. MALDI-TOF MS Calcd for $C_{60}H_{47}B_2N_6O_2$ $[M+H]^+$ 905.4, Found 905.4. HRMS (ESI): calcd. For $C_{60}H_{47}B_2N_6O_4$ $[M+H]^+$ 905.3947; Found 905.3932.

DPP derivative 3: A mixture of **1** (233 mg, 0.30 mmol), 4-ethynylanisole (198 mg, 1.5 mmol), Cs_2CO_3 (255 mg, 1.3 mmol), $PdCl_2(MeCN)_2$ (6.2 mg, 0.024 mmol) and XPhos (22.9 mg, 0.048 mmol) in MeCN (15.0 mL) was stirred for 10 min at room temperature under nitrogen atmosphere. The mixture was heated at 80 °C for 24 h. After cooling to room temperature, the volatiles were evaporated to dryness in vacuo. A dark purple solid was isolated by column chromatography on silica gel using $CHCl_3$/EtOAc (20/1) as an eluent. The product was obtained by the recrystallization ($CHCl_3$/hexane), and dried under vacuum to obtain a dark purple solid (133 mg, 50%). ^{1}H NMR (400 MHz, $C_2D_2Cl_4$, 333 K) δ 3.83 (s, 6H), 6.90 (d, 4H, J = 8.4 Hz), 7.28-7.33 (m, 12H), 7.41 (d, 8H, J = 7.6 Hz), 7.50 (d, 4H, J = 9.2 Hz), 8.21 (d, 2H, J = 8.2 Hz), 8.41 (d, 2H, J = 8.4 Hz), 8.48 (s, 2H); ^{13}C{^{1}H} NMR (100 MHz, $C_2D_2Cl_4$, 383 K) δ 55.3, 79.6, 99.5, 114.3, 114.4, 120.2, 123.2, 125.1, 126.9, 127.5, 127.7, 130.8, 132.8, 133.3, 133.6, 134.3, 139.0 145.2, 151.7; MALDI-TOF MS Calcd for $C_{58}H_{41}B_2N_4O_4$ $[M+H]^+$ 879.3, Found 879.4. HRMS (ESI): calcd. For $C_{58}H_{41}B_2N_4O_4$ $[M+H]^+$ 879.3314; Found 879.3332.

ACKNOWLEDGEMENTS

The authors thank the Chemical Analysis Center of the University of Tsukuba for the measurements of NMR, MALDI-TOF-MS, and ESI-MS.

REFERENCES

1. (a) C. Jiao, L. Zhu, and J. Wu, *Chem. Eur. J.*, 2011, **17**, 6610; (b) Y. Wu, C. Cheng, L. Jiao, C. Yu, S. Wang, Y. Wei, X. Mu, and E. Hao, *Org. Lett.*, 2014, **16**, 748.
2. (a) C. L. Amiot, S. Xu, S. Liang, L. Pan, and J. X. Zhao, *Sensors*, 2008, **8**, 3082; (b) K. Kiyose, H. Kojima, and T. Nagano, *Chem. Asian J.*, 2008, **3**, 506.
3. M. Grätzel, *J. Photochem. Photobiol. C*, 2003, **4**, 145.
4. G. Ulrich, R. Ziessel, and A. Harriman, *Angew. Chem. Int. Ed.*, 2008, **47**, 1184.
5. K. Umezawa, D. Citterio, and K. Suzuki, *Chem. Lett.*, 2007, **36**, 1424.
6. (a) H. He and D. K. P. Ng, *Org. Biomol. Chem.*, 2011, **9**, 2610; (b) S. Niu, G. Ulrich, P. Retailleau, and R. Ziessel, *Org. Lett.*, 2011, **13**, 4996.
7. (a) J. W. Jung, F. Liu, T. P. Russell, and W. H. Jo, *Chem. Commun.*, 2013, **49**, 8495; (b) Y. Deng, Y. Chem, J. Liu, L. Liu, H. Tian, Z. Xie, Y. Geng, and F. Wang, *ACS Appl. Mater. Interfaces*, 2013, **5**, 5741; (c) M. A. Naik and S. Patil, *J. Polym. Sci. A. Polym. Chem.*, 2013, **51**, 4241; (d) C. B. Nielsen, R. S. Ashraf, B. C. Schroeder, P. D'Angelo, S. E. Watkins, K. Song, T. D. Anthopoulos, and I. McCulloch, *Chem. Commun.*, 2012, **48**, 5832; (e) S. Qu and H. Tian, *Chem. Commun.*, 2012, **48**, 3039.
8. (a) B. Tieke, A. R. Rabindranath, K. Zhang, and Y. Zhu, *Beilstein J. Org. Chem.*, 2010, **6**, 830; (b) Y. Suna, J.-i. Nishida, Y. Fujisaki, and Y. Yamashita, *Chem. Lett.*, 2011, **40**, 822; (c) Y. Qiao, Y. Guo, C. Yu, F. Zhang, W. Xu, Y. Liu, and D. Zhu, *J. Am. Chem. Soc.*, 2012, **134**, 4084; (d) Y. Suna, J.-i. Nishida, Y. Fujisaki, and Y. Yamashita, *Org. Lett.*, 2012, **14**, 3356; (e) S.-Y. Liu, H.-Y. Li, M.-M. Shi, H. Jiang, X.-L. Hu, W.-Q. Li, L. Fu, and H.-Z. Chen, *Macromolecules*, 2012, **45**, 9004; (f) H. Liu, H. Jia, L. Wang, Y. Wu, C. Zhan, H. Fu, and J. Yao, *Phys. Chem. Chem. Phys.*, 2012, **14**, 14262.
9. T. Yamagata, J. Kuwabara, and T. Kanbara, *Tetrahedron Lett.*, 2010, **51**, 1596.
10. (a) S. Schutting, S. M. Borisov, and I. Klimant, *Anal. Chem.*, 2013, **85**, 3271; (b) G. Zhang, H. Li, S. Bi, L. Song, Y. Lu, L. Zhang, J. Yu, and L. Wang, *Analyst*, 2013, **138**, 6163; (c) G. Zhang, S. Bi, L. Song, F. Wang, J. Yu, and L. Wang, *Dyes Pigm.*, 2013, **99**, 779; (d) Y.-H. Jeong, C.-H. Lee, and W.-D. Jang, *Chem. Asian J.*, 2012, **7**, 1562; (e) C. Yang, M. Zheng, Y. Li, B. Zhang, J. Li, L. Bu, W. Liu, M. Sun, H. Zhang, Y. Tao, S. Xue, and W. Yang, *J. Mater. Chem. A*, 2013, **1**, 5172; (f) Y. Qu, S. Qu, L. Yang, J. Hua, and D. Qu, *Sensor and Actuators B*, 2012, **173**, 225.
11. M. Fukuda, K. Kodama, H. Yamamoto, and K. Mito, *Dyes Pigm.*, 2004, **63**, 115.
12. (a) G. M. Fischer, A. P. Ehlers, A. Zumbusch, and E. Daltrozzo, *Angew. Chem. Int. Ed.*, 2007, **46**,

3750; (b) G. M. Fischer, M. Isomäki-Krondahl, I. Göttker-Schnetmann, E. Daltrozzo, and A. Zumbusch, *Chem. Eur. J.*, 2009, **15**, 4857; (c) G. M. Fischer, M. K. Klein, E. Daltrozzo, and A. Zumbusch, *Eur. J. Org. Chem.*, 2011, 3421; (d) M. Y. Berezin, W. J. Akers, K. Guo, G. M. Fischer, E. Daltrozzo, A. Zumbusch, and S. Achilefu, *Biophys. J.*, 2009, **97**, L22; (e) G. M. Fischer, C. Jüngst, M. Isomäki-Krondahl, D. Gauss, H. M. Möller, E. Daltrozzo, and A. Zumbusch, *Chem. Commun.*, 2010, **46**, 5289; (f) S. Wiktorowski, G. M. Fischer, M. J. Winterhalder, E. Daltrozzo, and A. Zumbusch, *Phys. Chem. Chem. Phys.*, 2012, **14**, 2921.

13. S. Shimizu, T. Iino, Y. Araki, and N. Kobayashi, *Chem. Commun.*, 2013, **49**, 1621.
14. T. Yamagata, J. Kuwabara, and T. Kanbara, *Tetrahedron*, 2014, **70**, 1451.
15. O. Wallquist and R. Lenz, *Macromol. Symp.*, 2002, **187**, 617.
16. (a) J. Kuwabara, T. Yamagata, and T. Kanbara, *Tetrahedron*, 2010, **66**, 3736; (b) T. Yamagata, J. Kuwabara, and T. Kanbara, *Eur. J. Org. Chem.*, 2012, 5282.
17. (a) S. Luňák, Jr., J. Vyňuchal, M. Vala, L. Havel, and R. Hrdina, *Dyes Pigm.*, 2009, **82**, 102; (b) M. Vala, J. Vyňuchal, P. Toman, M. Weiter, and S. Luňák, Jr., *Dyes Pigm.*, 2010, **84**, 176; (c) M. Vala, M. Weiter, J. Vyňuchal, P. Toman, and S. Luňák, Jr., *J. Fluoresc.*, 2008, **18**, 1181.
18. Gaussian 09, Revision B.01, M. J. Frisch, G. W. Trucks, H. B. Schlegel, G. E. Scuseria, M. A. Robb, J. R. Cheeseman, G. Scalmani, V. Barone, B. Mennucci, G. A. Petersson, H. Nakatsuji, M. Caricato, X. Li, H. P. Hratchian, A. F. Izmaylov, J. Bloino, G. Zheng, J. L. Sonnenberg, M. Hada, M. Ehara, K. Toyota, R. Fukuda, J. Hasegawa, M. Ishida, T. Nakajima, Y. Honda, O. Kitao, H. Nakai, T. Vreven, J. A. Montgomery, Jr., J. E. Peralta, F. Ogliaro, M. Bearpark, J. J. Heyd, E. Brothers, K. N. Kudin, V. N. Staroverov, R. Kobayashi, J. Normand, K. Raghavachari, A. Rendell, J. C. Burant, S. S. Iyengar, J. Tomasi, M. Cossi, N. Rega, J. M. Millam, M. Klene, J. E. Knox, J. B. Cross, V. Bakken, C. Adamo, J. Jaramillo, R. Gomperts, R. E. Stratmann, O. Yazyev, A. J. Austin, R. Cammi, C. Pomelli, J. W. Ochterski, R. L. Martin, K. Morokuma, V. G. Zakrzewski, G. A. Voth, P. Salvador, J. J. Dannenberg, S. Dapprich, A. D. Daniels, Ö. Farkas, J. B. Foresman, J. V. Ortiz, J. Cioslowski, and D. J. Fox, Gaussian, Inc., Wallingford CT, 2009.
19. E. Q. Guo, P. H. Ren, Y. L. Zhang, H. C. Zhang, and W. J. Yang, *Chem. Commun.*, 2009, 5859.
20. I. Abrunhosa, L. Delain-Bioton, A.-C. Gaumont, M. Gulea, and S. Masson, *Tetrahedron*, 2004, **60**, 9263.